Research Square

Preprints are preliminary reports that have not undergone peer review.
They should not be considered conclusive, used to inform clinical practice,
or referenced by the media as validated information.

The Unit Two-Parameter Chris–Jerry Distribution: Properties and Applications

Riyas M

riyasm9747747497@gmail.com

Annamalai University

M Vijayakumar

Annamali University

Research Article

Keywords: Two parameter Chris–Jerry distribution, Hazard rate function, Entropy, Extropy, Inequality measures, Maximum likelihood estimation, Ordinary least squares estimation, Weighted least squares estimation.

Posted Date: November 18th, 2026

DOI: https://doi.org/10.21203/rs.3.rs-11768709/v1

License: This work is licensed under a Creative Commons Attribution 4.0 International License.
Read Full License

Additional Declarations: The authors declare no competing interests.

The Unit Two-Parameter Chris–Jerry Distribution: Properties and Applications

M. Riyas [1,a], M. Vijayakumar[1]

[1]Department of Statistics, Annamalai University, Annamalainagar 608002, Tamil Nadu, India.

[a]corresponding author: riyasm9747747497@gmail.com

Abstract: A bounded version of the two parameter Chris-Jerry distribution, referred to as the unit two parameter Chris-Jerry distribution, is introduced in this study. A comprehensive investigation of its important properties is carried out, including shape analysis, incomplete moments, moment generating function, hazard rate function and identifiability. Additionally, Shannon entropy, extropy, and inequality measures are derived to further characterize the proposed distribution. For parameter estimation, the methods of maximum likelihood estimation, least squares estimation, and weighted least squares estimation are employed. The performance of these estimators is evaluated through a simulation study. Finally, the applicability and effectiveness of the proposed model are demonstrated using two real datasets from different fields.

Keywords: Two parameter Chris–Jerry distribution, Hazard rate function, Entropy, Extropy, Inequality measures, Maximum likelihood estimation, Ordinary least squares estimation, Weighted least squares estimation.

1 Introduction

Many probability distributions have been proposed in the statistical literature to describe real-world phenomena across diverse disciplines. A large volume of these models are defined on the positive real line or the entire real line, and they have been extensively explored in both theoretical and applied perspectives. However, in several applied fields such as economics, medicine, biology, and engineering, the observed data are often naturally confined to a finite interval. Such observations typically arise in the form of proportions, rates, indices, and scores, thereby requiring statistical models that are specifically defined

on bounded supports. Although bounded data occur frequently in real applications, the number of distributions designed for such data is still limited compared to those defined on unbounded ranges. To overcome this limitation, recently researchers have proposed several new bounded distributions, mainly by applying transformation techniques to the well-known existing models, specifically focusing on proposing distributions bounded on $(0, 1)$.

For modeling data restricted to the unit interval, the Beta distribution is one of the most widely employed probability distributions [1]. Another important distribution for unit interval data is the Kumaraswamy distribution, which was introduced by [2].[3] advocated the use of the Kumaraswamy distribution as an alternative to the Beta distribution, owing to its several mathematically tractable properties and analytical advantages. In recent years, several new distributions have been developed to further enhance modeling capability and provide greater adaptability in analyzing data restricted to the unit interval. These include unit-inverse Gaussian distribution (UIG) [7], unit Muth distribution (UMD) [8], unit Teissier distribution (UTD) [9], unit linear failure rate distribution (ULFRD) [10], unit-modified Weibull distribution (UMWD) [11], and unit-Chen distribution (UCD) [12].Consequently, considerable advances have been made in the development of unit interval distributions, reflecting their increasing importance in statistical modeling. Nevertheless, the diverse characteristics of bounded data make it difficult for a single distribution to adequately accommodate all possible data patterns.

In this paper, we propose a new bounded distribution by adopting the two parameter Chris–Jerry distribution (TPCJD) coined by [13] as the baseline model. A continuous random variable (rv) X is said to follow the TPCJD with parameters $\lambda > 0,\ \theta > 0$ if its probability density function (pdf) is given by

$$f(x;\theta) = \frac{\theta^2}{\lambda\theta + 2}\left(\lambda + \theta x^2\right) e^{-\theta x}, \quad x > 0,\ \theta > 0. \tag{1}$$

The corresponding cumulative distribution function (cdf) is given by

$$F(x;\theta) = 1 - \frac{1}{\lambda\theta + 2}(\theta^2 x^2 + 2\theta x + \theta\lambda + 2)e^{-\theta x}, \quad x > 0,\ \theta > 0. \tag{2}$$

[13] introduced the TPCJD as an extension of the Chris–Jerry Distribution (CJD) proposed by [14]. The TPCJD was developed to provide a more flexible framework for modelling and analysing certain reliability and lifetime datasets. In addition to its theoretical flexibility, the estimation of its parameters can be readily addressed from both conventional and Bayesian perspectives. Subsequently, several researchers have investigated and extended the TPCJD, demonstrating its applicability across a variety of statistical domains. Among these contributions, [15] proposed a novel two-parameter model for modelling overdispersed count data by combining the TPCJD with the Pois-

son distribution. The proposed model enhances the flexibility of modeling integer-valued count time series and extends its applicability to statistical quality control for detecting increases in the mean of autocorrelated count processes. Its effectiveness is demonstrated through a real-world data application. Similarly, [16] developed a more flexible extension, termed the Generalized Weighted Chris–Jerry Distribution, and investigated its theoretical properties as well as its applicability in practical settings. The continued development and application of the TPCJD highlight its potential for flexible statistical modeling. Motivated by the growing need for flexible probability models for bounded data, we extend the TPCJD to the unit interval and introduce a corresponding bounded variant of the TPCJD.

Just as some real-life datasets defined on the positive real line exhibit a bathtub-shaped hazard rate function (HRF), certain datasets defined on the unit interval also exhibit a bathtub-shaped HRF. Considerable efforts have been devoted to enriching the existing literature for proposing distribution defined on both positive real line as well as unit intervals. For the sake of brevity, the literature survey concerning the extensions and generalizations of distributions supported on the positive real line is omitted here. Regarding the latter, the unit generalized half-normal distribution was recently introduced by [17]. However, it lacks closed-form expressions for its cumulative distribution function (CDF) and quantile function.

Some probability distributions defined on the unit interval, such as the unit Muth distribution [8], the unit exponential delay-time distribution [18], and unit J-shaped distributions [19], are known to exhibit bathtub-shaped HRFs. However, these distributions may not adequately capture the ideal bathtub shape of the HRF, as the resulting curve may be more appropriately characterized as V-shaped [20]. In contrast, an ideal model with a bathtub-shaped HRF should exhibit a prolonged and nearly constant, or flat, region between the initial decreasing phase and the subsequent increasing phase. The flat region of the bathtub-shaped HRF is of considerable practical importance in many real-world applications, thereby highlighting the need for models capable of accurately representing this feature. A notable example is the failure rate of integrated circuits, which typically exhibits a bathtub-shaped pattern with an extended flat region. The initial decreasing portion of the curve, corresponding to early-life failures, is primarily attributed to defects arising from material handling, manufacturing processes, and other production-related imperfections. These defects can result in a relatively high failure rate during the early stages of the product's life, followed by a decline as defective units are removed from the population. The subsequent increasing portion of the bathtub-shaped curve is generally associated with cumulative damage, wear, and natural degradation of the components over time. Accurate modelling of the bathtub-shaped HRF, particularly its extended flat region, is consequently essential for effective reliability analysis and decision-making. This highlights the importance of developing flexible life distri-

butions capable of adequately capturing the diverse shapes and characteristics of the bathtub-shaped hazard rate. This constitutes the primary motivation for developing and investigating a model capable of exhibiting an ideal bathtub-shaped HRF.

In this context, the proposed UTPCJD provides a simple and flexible alternative for modeling data on the unit interval. The UTPCJD has the advantage of having a simple pdf and allowing closed-form expressions for key statistical measures. Moreover, the UTPCJD is capable of exhibiting a bathtub-shaped hrf with long flat region, making it suitable for modeling real-life data with non-monotone behavior. Due to its simplicity, flexibility, and tractability, the UTPCJD offers an effective and practical model for bounded data.

The rest of this paper is settled in the following way. Section 2 introduces UTPCJD and discusses its important statistical properties, including shape analysis, identifiability, moments, incomplete moments and hrf. The Shannon entropy, extropy and inequality measures are derived in Section 3. In Section 4, parameter estimation methods such as maximum likelihood (ML) estimation, ordinary least squares (OLS), and weighted least squares (WLS) are presented. A simulation study is conducted in Section 5 to evaluate the performance of the estimators. Section 6 illustrates the applicability of the proposed model using two real datasets. Finally, Section 7 concludes the paper.

2 The Unit Two Parameter Chris–Jerry Distribution

In this section, UTPCJD is introduced, and some of its fundamental statistical properties are derived.

2.1 The proposed UTPCJD

The UTPCJD is obtained through the transformation $Y = e^{-X}$, based on the pdf of the TPCJD. Its formal definition is given as follows.

Definition 1. A rv Y is said to follow the UTPCJD with parameters $\theta > 0$, $\lambda > 0$, if its pdf is given by the following form:

$$f(y;\theta,\lambda) = \frac{\theta^2}{\lambda\theta+2} y^{\theta-1}(\lambda + \theta(\ln y)^2) \; ; \; y \in (0,1). \tag{3}$$

The corresponding cdf is given by

$$F(y;\theta,\lambda) = \frac{\theta^2}{\lambda\theta+2} y^{\theta} \left[(\ln y)^2 - \frac{2\ln y}{\theta} + \frac{\lambda}{\theta} + \frac{2}{\theta^2} \right]. \tag{4}$$

2.2 Shape and mode

The following result characterizes the shape and mode of the UTPCJD.

Result 1. The pdf of the UTPCJD attains its mode at

$$y_{mode} = \exp\left(\frac{-\theta + \sqrt{\theta^2 - \lambda\theta(\theta-1)^2}}{\theta(\theta-1)}\right). \tag{5}$$

Proof. To find the mode, take the logarithm of (3):

$$\ln(f(y;\theta,\lambda)) = \ln\left(\frac{\theta^2}{\lambda\theta+2}\right) + (\theta-1)\ln(y) + \ln(\lambda + \theta(\ln(y))^2),$$

Differentiate $\ln(f(y;\theta,\lambda))$ with respect to y to obtain:

$$\frac{d\ln(f(y;\theta,\lambda))}{dy} = \frac{1}{y}\left[(\theta-1) + \frac{2\theta\ln(y)}{\lambda+\theta(\ln(y))^2}\right],$$

Equating this equation to zero and solving for y, we obtain

$$y_{mode} = \exp\left(\frac{-\theta + \sqrt{\theta^2 - \lambda\theta(\theta-1)^2}}{\theta(\theta-1)}\right). \tag{6}$$

To illustrate the behavior of the distribution, plots of the pdf for various values of θ and λ are provided in Figure 1.

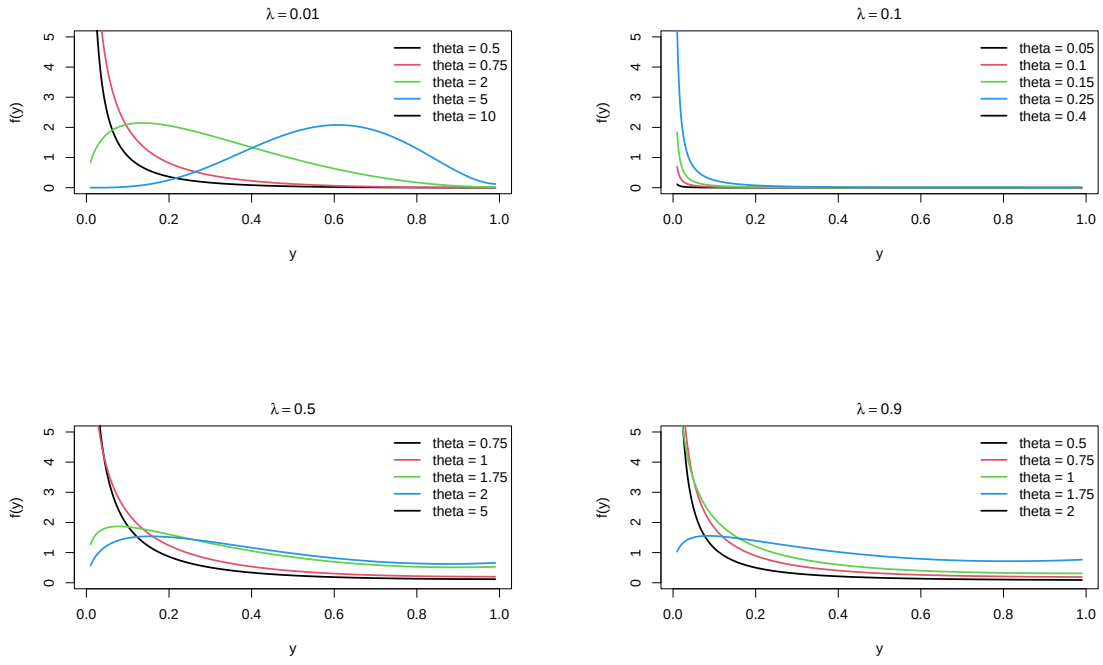


Figure 1: Plots of the pdf of the UTPCJD for different values of λ and θ.

2.3 Identifiability

The problem of identifiability (see [6]) lies in the uniqueness of distribution for the unknown parameters in the model. That is, the parameters should uniquely determine a distribution. The set of unknown parameters of a particular model is said to be identifiable, if different sets of parameters give different distributions for a given y.

Here the identifiability property of UTPCJD is verified. Let f_{Λ_1,Θ_1} and $f_{\Lambda_2\Theta_2}$ be different members of UTPCJD indexed by $\Theta_1 = \theta_1$, $\Theta_2 = \theta_2$ and $\Lambda_1 = \lambda_1$, $\Lambda_2 = \lambda_2$ respectively. Then the likelihood ratio:

$$\begin{aligned} L &= \frac{f(y;\lambda_1,\theta_1)}{f(y;\lambda_2,\theta_2)}, \\ &= \frac{\dfrac{\theta_1^2}{\lambda_1\theta_1+2}\left(\lambda_1+\theta_1(\ln y)^2\right)y^{\theta_1-1}}{\dfrac{\theta_2^2}{\lambda_2\theta_2+2}\left(\lambda_2+\theta_2(\ln y)^2\right)y^{\theta_2-1}}, \\ &= \frac{\theta_1^2(\lambda_2\theta_2+2)}{\theta_2^2(\lambda_1\theta_1+2)}\cdot y^{\theta_1-\theta_2}\cdot\frac{\lambda_1+\theta_1(\ln y)^2}{\lambda_2+\theta_2(\ln y)^2}. \end{aligned}$$

Taking log on both sides:

$$\log L = \log\left(\frac{\theta_1^2(\lambda_2\theta_2+2)}{\theta_2^2(\lambda_1\theta_1+2)}\right) + (\theta_1-\theta_2)\log y + \log(\lambda_1+\theta_1(\ln y)^2) - \log(\lambda_2+\theta_2(\ln y)^2).$$

Differentiate w.r.t y, and equating to 0, we get

$$\frac{d}{dy}\log L = 0 \quad\Longrightarrow\quad \frac{\theta_1-\theta_2}{y} + \frac{2\theta_1\ln y}{y\left(\lambda_1+\theta_1(\ln y)^2\right)} - \frac{2\theta_2\ln y}{y\left(\lambda_2+\theta_2(\ln y)^2\right)} = 0.$$

This holds for all $y \in (0,1)$. By comparing the constant terms,

$$\theta_1-\theta_2 = 0 \implies \theta_1 = \theta_2 = \theta.$$

On substituting $\theta_1 = \theta_2 = \theta$ into the above equation, we get

$$\begin{aligned} \frac{2\theta\ln y}{\lambda_1+\theta(\ln y)^2} &= \frac{2\theta\ln y}{\lambda_2+\theta(\ln y)^2}, \\ \frac{1}{\lambda_1+\theta(\ln y)^2} &= \frac{1}{\lambda_2+\theta(\ln y)^2}, \\ \lambda_1+\theta(\ln y)^2 &= \lambda_2+\theta(\ln y)^2, \\ \lambda_1 &= \lambda_2. \end{aligned}$$

The above equality holds for all $y \in (0,1)$ if and only if $\theta_1 = \theta_2$ and $\lambda_1 = \lambda_2$. Hence, the parameters uniquely determine the corresponding distribution. Therefore, the UTPCJD is identifiable; that is, $f_{\Lambda_1,\Theta_1}(y) = f_{\Lambda_2,\Theta_2}(y) \Longleftrightarrow \Theta_1 = \Theta_2$ and $\Lambda_1 = \Lambda_2$.

2.4 Moments

The following result provides the moments of the UTPCJD.

Result 2. For any non-negative integer r, the r^{th} non-central moment of a rv Y following the UTPCJD is given by

$$\mu'_r = E(Y^r) = \frac{\theta^2}{\lambda\theta + 2}\left[\frac{\lambda}{\theta + r} + \frac{2\theta}{(\theta + r)^3}\right]. \tag{7}$$

Proof. Using the definition of the non-central moment together with the pdf of the UTPCJD, we have

$$\begin{aligned}
\mu'_r &= \int_0^1 y^r f(y;\theta,\lambda)\, dy \\
&= \int_0^1 y^r \frac{\theta^2}{\lambda\theta + 2} y^{\theta-1}\left(\lambda + \theta(\ln y)^2\right)\, dy \\
&= \frac{\theta^2}{\lambda\theta + 2}\left[\frac{\lambda}{\theta + r} + \frac{2\theta}{(\theta + r)^3}\right].
\end{aligned}$$

Result 3. If $Y \sim \text{UTPCJD}(\theta)$, then the mean and variance are given by

$$E(Y) = \frac{\theta^2}{\lambda\theta + 2}\left[\frac{\lambda}{\theta + 1} + \frac{2\theta}{(\theta + 1)^3}\right]. \tag{8}$$

$$\text{Var}(Y) = \frac{\theta^2}{\lambda\theta + 2}\left(\frac{\lambda}{\theta + 2} + \frac{2\theta}{(\theta + 2)^3}\right) - \left[\frac{\theta^2}{\lambda\theta + 2}\left(\frac{\lambda}{\theta + 1} + \frac{2\theta}{(\theta + 1)^3}\right)\right]^2. \tag{9}$$

Proof. The mean is obtained from Result 2 by setting $r = 1$ and substituting the pdf of UTPCJD. Thus, we obtain

$$\begin{aligned}
E(Y) &= \int_0^1 y \cdot f(y;\theta,\lambda)\, dy, \\
&= \frac{\theta^2}{\lambda\theta + 2}\left[\frac{\lambda}{\theta + 1} + \frac{2\theta}{(\theta + 1)^3}\right].
\end{aligned}$$

and

$$Var(Y) = E(Y^2) - [E(Y)]^2.$$

Substituting $r = 2$ in (7), we obtain

$$E(Y^2) = \frac{\theta^2}{\lambda\theta + 2}\left[\frac{\lambda}{\theta + 2} + \frac{2\theta}{(\theta + 2)^3}\right].$$

Therefore,

$$\mathrm{Var}(Y) = \frac{\theta^2}{\lambda\theta+2}\left(\frac{\lambda}{\theta+2}+\frac{2\theta}{(\theta+2)^3}\right) - \left[\frac{\theta^2}{\lambda\theta+2}\left(\frac{\lambda}{\theta+1}+\frac{2\theta}{(\theta+1)^3}\right)\right]^2.$$

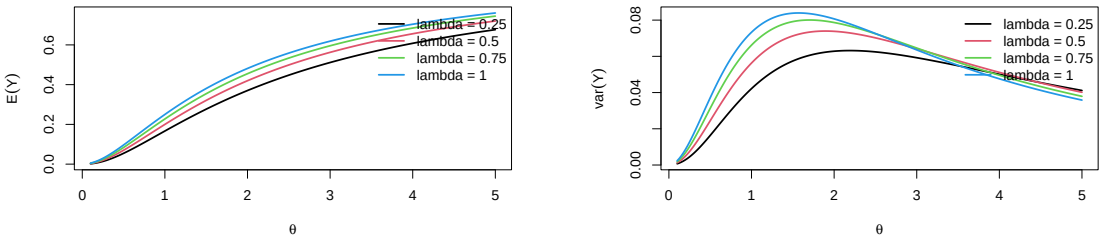


Figure 2: Mean and variance of the UTPCJD for different values of λ and θ.

Result 4. Let Y be a rv following the UTPCJD with parameter $\lambda > 0,\ \theta > 0$. Then, the skewness and kurtosis are given by

$$\mathrm{skewness}(Y) = \gamma_1 = \frac{\frac{\theta^2}{\lambda\theta+2}\left[\frac{\lambda}{\theta+3}+\frac{2\theta}{(\theta+3)^3}\right] - 3\cdot\frac{\theta^2}{\lambda\theta+2}\left[\frac{\lambda}{\theta+1}+\frac{2\theta}{(\theta+1)^3}\right]}{\left[\frac{\theta^2}{\lambda\theta+2}\left(\frac{\lambda}{\theta+2}+\frac{2\theta}{(\theta+2)^3}\right)\right] + 2\left[\frac{\theta^2}{\lambda\theta+2}\left(\frac{\lambda}{\theta+1}+\frac{2\theta}{(\theta+1)^3}\right)\right]^3}{\left[\frac{\theta^2}{\lambda\theta+2}\left(\frac{\lambda}{\theta+2}+\frac{2\theta}{(\theta+2)^3}\right) - \left(\frac{\theta^2}{\lambda\theta+2}\left(\frac{\lambda}{\theta+1}+\frac{2\theta}{(\theta+1)^3}\right)\right)^2\right]^{3/2}}$$

and

$$\mathrm{kurtosis}(Y) = \gamma_2 = \frac{\frac{\theta^2}{\lambda\theta+2}\left[\frac{\lambda}{\theta+4}+\frac{2\theta}{(\theta+4)^3}\right] - 4\left[\frac{\theta^2}{\lambda\theta+2}\left(\frac{\lambda}{\theta+1}+\frac{2\theta}{(\theta+1)^3}\right)\right]}{\left[\frac{\theta^2}{\lambda\theta+2}\left(\frac{\lambda}{\theta+3}+\frac{2\theta}{(\theta+3)^3}\right)\right] + 6\left[\frac{\theta^2}{\lambda\theta+2}\left(\frac{\lambda}{\theta+1}+\frac{2\theta}{(\theta+1)^3}\right)\right]^2}{\left[\frac{\theta^2}{\lambda\theta+2}\left(\frac{\lambda}{\theta+2}+\frac{2\theta}{(\theta+2)^3}\right)\right] - 3\left[\frac{\theta^2}{\lambda\theta+2}\left(\frac{\lambda}{\theta+1}+\frac{2\theta}{(\theta+1)^3}\right)\right]^4}{\left[\frac{\theta^2}{\lambda\theta+2}\left(\frac{\lambda}{\theta+2}+\frac{2\theta}{(\theta+2)^3}\right) - \left(\frac{\theta^2}{\lambda\theta+2}\left(\frac{\lambda}{\theta+1}+\frac{2\theta}{(\theta+1)^3}\right)\right)^2\right]^2}.$$

Proof. Based on Result 2, we can easily obtain skewness and kurtosis of UTPCJD.

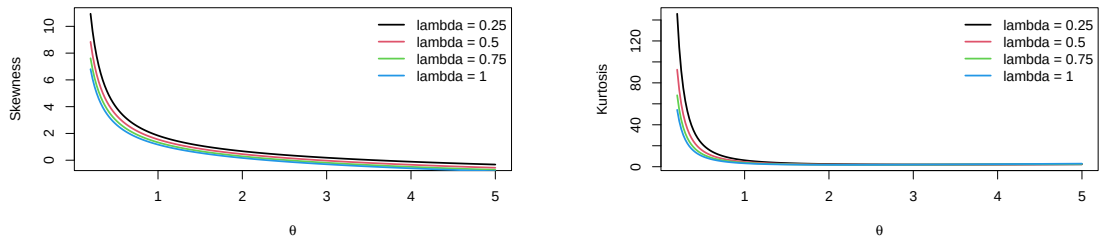


Figure 3: Skewness and kurtosis of the UTPCJD for different values of λ and θ.

2.5 Moment Generating Function

In this subsection, the moment generating function (mgf) of the UTPCJD are derived.

Result 5. Let $Y \sim \text{UTPCJD}(\lambda, \theta)$, where $\lambda > 0,\ \theta > 0$. Then, the mgf is given by

$$M_Y(t) = \frac{\theta^2}{\lambda\theta + 2} \sum_{r=0}^{\infty} \frac{t^r}{r!} \left[\frac{\lambda}{r+\theta} + \frac{2\theta}{(r+\theta)^3} \right].$$

Proof. Based on the definition of mgf we have,

$$M_Y(t) = E(e^{tY}) = \int_0^1 e^{ty} \cdot f_Y(y; \lambda, \theta)\, dy.$$

Substituting the pdf of the UTPCJD and the expression for e^{ty} into the above equation, we obtain

$$M_Y(t) = \frac{\theta^2}{\lambda\theta + 2} \sum_{r=0}^{\infty} \frac{t^r}{r!} \left[\frac{\lambda}{r+\theta} + \frac{2\theta}{(r+\theta)^3} \right].$$

Thus, the proof is complete.

2.6 Incomplete Moments

In this subsection, a closed-form expression for the incomplete moments of the UTPCJD is derived.

Result 6. Let Y be a rv following the UTPCJD. For $r = 1, 2, \ldots$, the r^{th} incomplete moment is given by

$$m_r(t, \lambda, \theta) = \frac{\theta^2 t^{r+\theta}}{\lambda\theta + 2(r+\theta)} \left[\lambda + \theta(\ln t)^2 - \frac{2\ln t}{\theta + r} + \frac{2}{(r+\theta)^2} \right].$$

Proof. From the definition of the incomplete moment, we have

$$m_r(t,\lambda,\theta) = \int_0^t y^r f(y)\, dy.$$

Substituting the pdf of the UTPCJD into the above integral and evaluating the resulting integral, we obtain

$$m_r(t,\lambda,\theta) = \frac{\lambda\theta^2 t^{r+\theta}}{\theta + 2(r+\theta)} \left[\lambda + \theta((\ln t)^2 - \frac{2\ln t}{r+\theta} + \frac{2}{(r+\theta)^2})\right].$$

2.7 Hazard Rate Function

The HRF is an important characteristic in lifetime analysis and reliability theory. For example, in maintenance and replacement planning and also in resource allocation. It represents the instantaneous failure rate of a unit that has survived up to time y.

Result 7. Let $Y \sim \text{UTPCJD}(\lambda,\theta)$. Then, the HRF is given by

$$h(y) = \frac{\theta^2\,(\lambda + \theta(\ln y)^2)}{\dfrac{\lambda\theta+2}{y^{\theta-1}} - \theta^2 y(\ln y)^2 + 2\theta y \ln y - 2y - \lambda\theta y}.$$

Proof. Based on the definition of HRF, we have

$$h(y) = \frac{f(y)}{1 - F(y)}.$$

where $f(y)$ is the pdf of the UTPCJD and $F(y)$ is the cdf of the UTPCJD. Then, we obtain

$$\begin{aligned} h(y) &= \frac{\dfrac{\theta^2}{\lambda\theta+2}\,(\lambda + \theta(\ln y)^2)\, y^{\theta-1}}{1 - \dfrac{\theta^2}{\lambda\theta+2} y^\theta \left[(\ln y)^2 - \dfrac{2\ln y}{\theta} + \dfrac{2}{\theta^2} + \dfrac{\lambda}{\theta}\right]} \\ &= \frac{\theta^2\,(\lambda + \theta(\ln y)^2)}{\dfrac{\lambda\theta+2}{y^{\theta-1}} - y\,[\theta^2(\ln y)^2 - 2\theta\ln y + 2 + \lambda\theta]}. \end{aligned}$$

Thus, the proof is complete.

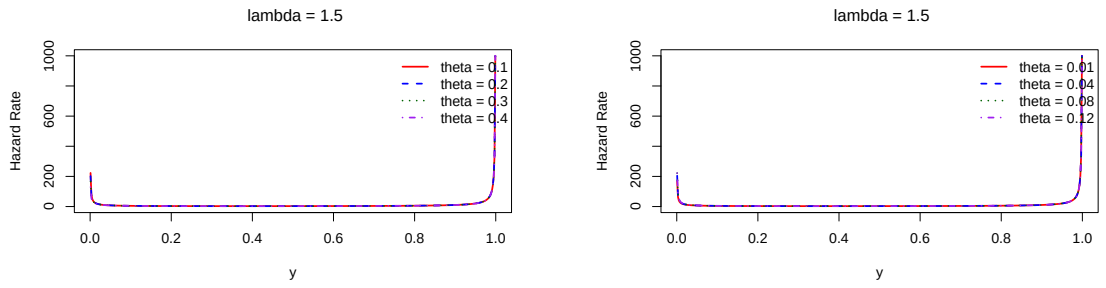


Figure 4: HRF plot of the UTPCJD for different values of λ and θ.

In Figure 4, the HRF displays a bathtub-shaped pattern, indicating a high initial failure rate that decreases over time, followed by a nearly constant region, and finally an increasing trend at later stages. This behavior reflects the different phases of failure, namely early failures, random failures, and wear-out failures. Such a shape provides greater flexibility in modeling lifetime data, allowing the distribution to capture a wide range of real-world failure patterns effectively.

3 Shannon Entropy, Extropy, and Inequality Measures

In this section, measures of uncertainty and inequality associated with the UTPCJD are studied, including Shannon entropy, extropy, and standard inequality measures.

3.1 Shannon Entropy

Shannon entropy [21] measures the uncertainty associated with a rv. For a continuous rv Y with pdf $f(y)$ on $(0, 1)$, it is defined as

$$H(Y) = -\int_0^1 f(y)\, \log f(y)\, dy.$$

Result 8. Let $Y \sim \text{UTPCJD}(\lambda, \theta)$. Then, the Shannon entropy associated with Y is given by

$$H(Y) = -\log\left(\frac{\theta^2}{\lambda\theta + 2}\right) - E\big[\log(\lambda + \theta(\ln Y)^2)\big] + \frac{(\theta - 1)(\lambda + 6)}{\lambda\theta + 2}.$$

Proof. Given,

$$\begin{aligned}
H(Y) &= -\int_0^1 f(y;\lambda,\theta)\log f(y;\lambda,\theta)\,dy,\\
&= -\int_0^1 \frac{\theta^2}{\lambda\theta+2}y^{\theta-1}(\lambda+\theta(\ln y)^2)\cdot\log\left[\frac{\theta^2}{\lambda\theta+2}y^{\theta-1}(\lambda+\theta(\ln y)^2)\right]dy,\\
&= -\log\left(\frac{\theta^2}{\lambda\theta+2}\right) - E\big[\log(\lambda+\theta(\ln Y)^2)\big] + (\theta-1)E(logY),\\
&= -\log\left(\frac{\theta^2}{\lambda\theta+2}\right) - E\big[\log(\lambda+\theta(\ln Y)^2)\big] + \frac{(\theta-1)(\lambda+6)}{\lambda\theta+2}.
\end{aligned}$$

Thus, the proof is complete.

3.2 Extropy

[22] introduced extropy as a complementary measure to Shannon entropy and it has several applications, including the evaluation of forecasting distributions, comparison of uncertainty between rvs, and modeling of physical phenomena. For a continuous rv Y with pdf $f(y)$ on $(0,1)$, the extropy is defined as

$$J(Y) = -\frac{1}{2}\int_0^1 f^2(y)\,dy. \tag{10}$$

Result 9. If $Y \sim$ UTPCJD(λ,θ), then the extropy is given by

$$J(Y) = -\frac{1}{2}\left(\frac{\theta^4}{(\lambda\theta+2)^2}\right)\left[\frac{\lambda^2}{2\theta-1} + \frac{4\lambda\theta}{(2\theta-1)^3} + \frac{24\theta^2}{(2\theta-1)^5}\right].$$

Proof. From the definition of extropy,

$$J(Y) = -\frac{1}{2}\int_0^1 f^2(y;\theta,\lambda)\,dy.$$

Substituting the pdf of the UTPCJD, we obtain

$$\int_0^1 f^2(y;\theta,\lambda)\,dy = \frac{\theta^4}{(\lambda\theta+2)^2}\left[\lambda^2\int_0^1 y^{2\theta-2}\,dy + 2\lambda\theta\int_0^1 y^{2\theta-2}(\ln y)^2\,dy + \theta^2\int_0^1 y^{2\theta-2}(\ln y)^4\,dy\right].$$

Evaluating the above integrals, we obtain

$$J(Y) = -\frac{1}{2}\left(\frac{\theta^4}{(\lambda\theta+2)^2}\right)\left[\frac{\lambda^2}{2\theta-1} + \frac{4\lambda\theta}{(2\theta-1)^3} + \frac{24\theta^2}{(2\theta-1)^5}\right].$$

Thus, the proof is attained.

3.3 Inequality Measures

Inequality measures such as Lorenz and Bonferroni curves [4] are widely used in economics, reliability analysis, medicine, and other applied disciplines to assess dispersion.

The Zenga curve [5] provides an additional measure of inequality. In this subsection, these measures are derived for the UTPCJD.

Lorenz curve. The Lorenz curve is defined as

$$L_F(y) = \frac{\int_0^y t f(t)\, dt}{E(Y)}.$$

For the UTPCJD, we have

$$\int_0^y t f(t)\, dt = \frac{\theta^2}{\lambda\theta + 2} \cdot \frac{y^{\theta+1}}{\theta+1}\big[\lambda + \theta\left((\ln y)^2 - \frac{2\ln y}{\theta+1} + \frac{2}{(\theta+1)^2}\right)\big],$$

and $E(Y)$ is given in equation (8).
Hence, the Lorenz curve simplifies to

$$L_F(y) = \frac{y^{\theta+1}\left[\lambda + \theta\left((\ln y)^2 - \frac{2\ln y}{\theta+1} + \frac{2}{(\theta+1)^2}\right)\right]}{\lambda + \frac{2\theta}{(\theta+1)^2}}.$$

Bonferroni curve. The Bonferroni curve is defined as

$$B_F(y) = \frac{\int_0^y t f(t)\, dt}{E(Y)F(y)}.$$

The Bonferroni curve of UTPCJD is obtained as

$$B_F(y) = \frac{y\left[\lambda + \theta\left((\ln y)^2 - \frac{2\ln y}{\theta+1} + \frac{2}{(\theta+1)^2}\right)\right]}{\left[\lambda + \frac{2\theta}{(\theta+1)^2}\right]\left[(\ln y)^2 - \frac{2\ln y}{\theta} + \frac{2}{\theta^2} + \frac{\lambda}{\theta}\right]}.$$

Zenga curve. The Zenga curve is defined as

$$A_F(y) = 1 - \frac{\mu^-(y)}{\mu^+(y)}.$$

The Zenga curve of UTPCJD is obtained as

$$A_F(y) = 1 - \frac{\dfrac{y\left[\lambda + \theta\left((\ln y)^2 - \dfrac{2\ln y}{\theta+1} + \dfrac{2}{(\theta+1)^2}\right)\right]}{(\theta+1)\left[(\ln y)^2 - \dfrac{2\ln y}{\theta} + \dfrac{2}{\theta^2} + \dfrac{\lambda}{\theta}\right]}}{\dfrac{\left[\dfrac{\lambda}{\theta+1} + \dfrac{2\theta}{(\theta+1)^3}\right] - \dfrac{y^{\theta+1}\left[\lambda + \theta\left((\ln y)^2 - \dfrac{2\ln y}{\theta+1} + \dfrac{2}{(\theta+1)^2}\right)\right]}{\theta+1}}{1 - y^{\theta}\left[(\ln y)^2 - \dfrac{2\ln y}{\theta} + \dfrac{2}{\theta^2} + \dfrac{\lambda}{\theta}\right]}}.$$

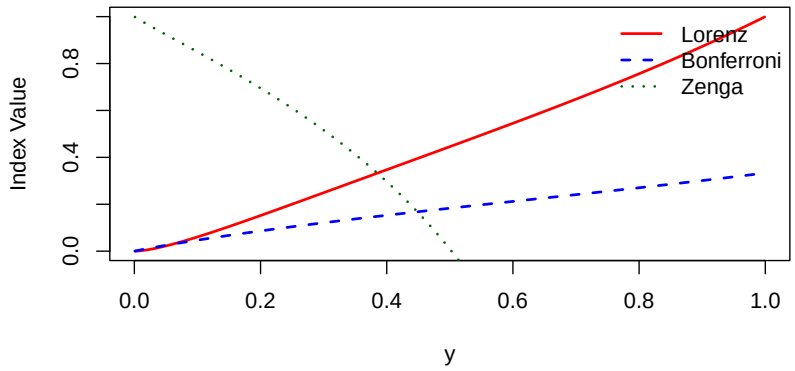


Figure 5: Lorenz, Bonferroni, and Zenga curves for the UTPCJD.

4 Parameter Estimation

This section presents the procedures used for estimating and making inferences about the parameters of the UTPCJD.

4.1 Maximum Likelihood Estimation

Let $y_1, y_2, \ldots, y_n$ be a random sample of size n drawn from the UTPCJD with parameters $\lambda > 0,\ \theta > 0$. The likelihood function is expressed as

$$L(\theta, \lambda) = \left(\frac{\theta^2}{\lambda\theta + 2}\right)^n \prod_{i=1}^{n} y_i^{\theta-1}\left(\lambda + \theta(\ln y_i)^2\right).$$

Taking the natural logarithm, the log-likelihood function becomes

$$\ell(\theta, \lambda) = 2n\ln\theta - n\ln(\lambda\theta + 2) + (\theta - 1)\sum_{i=1}^{n}\ln y_i + \sum_{i=1}^{n}\ln\left(\lambda + \theta(\ln y_i)^2\right).$$

The ML estimates, denoted by $\hat{\theta}$ and $\hat{\lambda}$, are obtained by maximizing the log-likelihood function. This leads to the following system of likelihood equations:

$$\frac{\partial \ell(\theta,\lambda)}{\partial \theta} = \frac{2n}{\theta} - \frac{n\lambda}{\lambda\theta+2} + \sum_{i=1}^{n} \ln y_i + \sum_{i=1}^{n} \frac{(\ln y_i)^2}{\lambda+\theta(\ln y_i)^2} = 0,$$

$$\text{and} \qquad \frac{\partial \ell(\theta,\lambda)}{\partial \lambda} = -\frac{n\theta}{\lambda\theta+2} + \sum_{i=1}^{n} \frac{1}{\lambda+\theta(\ln y_i)^2} = 0.$$

Since these equations do not admit explicit solutions, the ML estimates are computed using numerical optimization methods such as iterative algorithms implemented in statistical software like R.

4.2 Ordinary and Weighted Least-Squares Estimation

Let $y_{1:n}, y_{2:n}, \ldots, y_{n:n}$ denote the ordered observations of $y_1, y_2, \ldots, y_n$. The OLS estimators denoted by $(\tilde{\theta}, \tilde{\lambda})$, are obtained by minimizing the objective function

$$R(\theta,\lambda) = \sum_{i=1}^{n} \left[F(y_{i:n};\theta,\lambda) - \frac{i}{n+1} \right]^2.$$

These estimators can alternatively be derived by solving the system of equations

$$\frac{\partial R(\theta,\lambda)}{\partial \theta} = 0 \qquad \text{and} \qquad \frac{\partial R(\theta,\lambda)}{\partial \lambda} = 0,$$

where

$$\frac{\partial R(\theta,\lambda)}{\partial \theta} = 2\sum_{i=1}^{n} \left[F(y_{i:n};\theta,\lambda) - \frac{i}{n+1} \right] \frac{\partial F(y_{i:n};\theta,\lambda)}{\partial \theta},$$

$$\text{and} \qquad \frac{\partial R(\theta,\lambda)}{\partial \lambda} = 2\sum_{i=1}^{n} \left[F(y_{i:n};\theta,\lambda) - \frac{i}{n+1} \right] \frac{\partial F(y_{i:n};\theta,\lambda)}{\partial \lambda}.$$

In a similar manner, the WLS estimators denoted by $(\breve{\theta}, \breve{\lambda})$, are obtained by minimizing

$$W(\theta,\lambda) = \sum_{i=1}^{n} \frac{(n+1)^2(n+2)}{i(n-i+1)} \left[F(y_{i:n};\theta,\lambda) - \frac{i}{n+1} \right]^2.$$

The corresponding estimating equations are given by

$$\frac{\partial W(\theta,\lambda)}{\partial \theta} = 0, \qquad \frac{\partial W(\theta,\lambda)}{\partial \lambda} = 0.$$

As with the likelihood approach, closed-form solutions are not available. Therefore, the LSE and WLSE are obtained numerically using optimization techniques implemented through the **optim** function in **R**.

5 Simulation Study

A simulation study is conducted to assess the performance of the ML, OLS, and WLS estimators in estimating the parameters θ and λ. Samples are generated from the UT-PCJD for various combinations of parameter values and sample sizes. The performance of the estimators is evaluated based on their bias, mean squared error (MSE), and root mean squared error (RMSE).

Table 1: Simulation results for ML estimates, Bias, MSE and RMSE.

n	$\hat{\theta}$	$\hat{\lambda}$	Bias(θ)	Bias(λ)	MSE(θ)	MSE(λ)	RMSE(θ)	RMSE(λ)
			$\theta = 0.8,\ \lambda = 0.5$					
50	0.8070	0.5664	0.0070	0.0664	0.0068	0.1943	0.0826	0.4408
75	0.8074	0.5326	0.0074	0.0326	0.0050	0.1278	0.0706	0.3574
200	0.8030	0.5118	0.0030	0.0118	0.0019	0.0369	0.0440	0.1920
300	0.7990	0.5218	-0.0010	0.0218	0.0013	0.0255	0.0362	0.1596
500	0.8008	0.5072	0.0008	0.0072	0.0007	0.0140	0.0264	0.1184
1000	0.8004	0.4990	0.0004	-0.0010	0.0003	0.0068	0.0173	0.0827
			$\theta = 0.8,\ \lambda = 1.0$					
50	0.8110	1.1024	0.0110	0.1024	0.0107	0.5286	0.1033	0.7270
75	0.8067	1.0663	0.0067	0.0663	0.0064	0.3581	0.0797	0.5984
200	0.8057	1.0122	0.0057	0.0122	0.0025	0.1291	0.0504	0.3593
300	0.8011	1.0204	0.0011	0.0204	0.0017	0.0808	0.0407	0.2842
500	0.8017	1.0107	0.0017	0.0107	0.0010	0.0471	0.0314	0.2171
1000	0.8010	1.0042	0.0010	0.0042	0.0005	0.0221	0.0220	0.1486
			$\theta = 1.5,\ \lambda = 0.5$					
50	1.5142	0.5739	0.0142	0.0739	0.0326	0.2021	0.1807	0.4495
75	1.5189	0.5381	0.0189	0.0381	0.0220	0.1154	0.1482	0.3397
200	1.5025	0.5195	0.0025	0.0195	0.0088	0.0318	0.0937	0.1784
300	1.5023	0.5140	0.0023	0.0140	0.0061	0.0222	0.0784	0.1489
500	1.5050	0.5055	0.0050	0.0055	0.0031	0.0109	0.0559	0.1042
1000	1.5006	0.5049	0.0006	0.0049	0.0016	0.0053	0.0395	0.0730
			$\theta = 1.5,\ \lambda = 1.0$					
50	1.5238	1.1728	0.0238	0.1728	0.0529	0.6643	0.2300	0.8151
75	1.5186	1.1131	0.0186	0.1131	0.0344	0.4612	0.1854	0.6792
200	1.5103	1.0387	0.0103	0.0387	0.0135	0.1619	0.1160	0.4023
300	1.5033	1.0372	0.0033	0.0372	0.0085	0.0943	0.0921	0.3071
500	1.5005	1.0307	0.0005	0.0307	0.0055	0.0606	0.0742	0.2463
1000	1.5021	1.0073	0.0021	0.0073	0.0026	0.0253	0.0506	0.1590

Table 2: Simulation results for OLS estimates, Bias, MSE and RMSE.

n	$\hat{\theta}$	$\hat{\lambda}$	Bias(θ)	Bias(λ)	MSE(θ)	MSE(λ)	RMSE(θ)	RMSE(λ)
			$\theta = 0.8,\ \lambda = 0.5$					
50	0.7871	0.6827	-0.0129	0.1827	0.0084	0.3034	0.0916	0.5508
75	0.7927	0.6196	-0.0073	0.1196	0.0058	0.1996	0.0765	0.4468
200	0.7991	0.5314	-0.0009	0.0314	0.0023	0.0492	0.0481	0.2217
300	0.7958	0.5372	-0.0042	0.0372	0.0016	0.0364	0.0403	0.1907
500	0.7986	0.5212	-0.0014	0.0212	0.0008	0.0193	0.0291	0.1389
1000	0.7994	0.5056	-0.0006	0.0056	0.0004	0.0093	0.0199	0.0967
			$\theta = 0.8,\ \lambda = 1.0$					
50	0.7885	1.2746	-0.0115	0.2746	0.0124	0.7521	0.1114	0.8672
75	0.7904	1.1902	-0.0096	0.1902	0.0078	0.4884	0.0881	0.6989
200	0.7994	1.0567	-0.0006	0.0567	0.0031	0.1609	0.0555	0.4011
300	0.7975	1.0470	-0.0025	0.0470	0.0021	0.0996	0.0453	0.3156
500	0.7991	1.0291	-0.0009	0.0291	0.0012	0.0553	0.0346	0.2352
1000	0.8000	1.0111	0.0000	0.0111	0.0006	0.0259	0.0248	0.1608
			$\theta = 1.5,\ \lambda = 0.5$					
50	1.4654	0.6805	-0.0346	0.1805	0.0399	0.3044	0.1997	0.5517
75	1.4880	0.6019	-0.0120	0.1019	0.0261	0.1648	0.1616	0.4059
200	1.4900	0.5430	-0.0100	0.0430	0.0105	0.0421	0.1023	0.2051
300	1.4969	0.5264	-0.0031	0.0264	0.0073	0.0266	0.0853	0.1631
500	1.5002	0.5136	0.0002	0.0136	0.0037	0.0125	0.0609	0.1120
1000	1.4985	0.5085	-0.0015	0.0085	0.0018	0.0058	0.0426	0.0762
			$\theta = 1.5,\ \lambda = 1.0$					
50	1.4677	1.3822	-0.0323	0.3822	0.0601	0.9568	0.2452	0.9782
75	1.4800	1.2676	-0.0200	0.2676	0.0441	0.6841	0.2099	0.8217
200	1.4952	1.0915	-0.0048	0.0915	0.0163	0.2108	0.1278	0.4591
300	1.4924	1.0767	-0.0076	0.0767	0.0115	0.1299	0.1072	0.3604
500	1.4939	1.0537	-0.0061	0.0537	0.0070	0.0763	0.0840	0.2763
1000	1.5005	1.0139	0.0005	0.0139	0.0032	0.0295	0.0565	0.1717

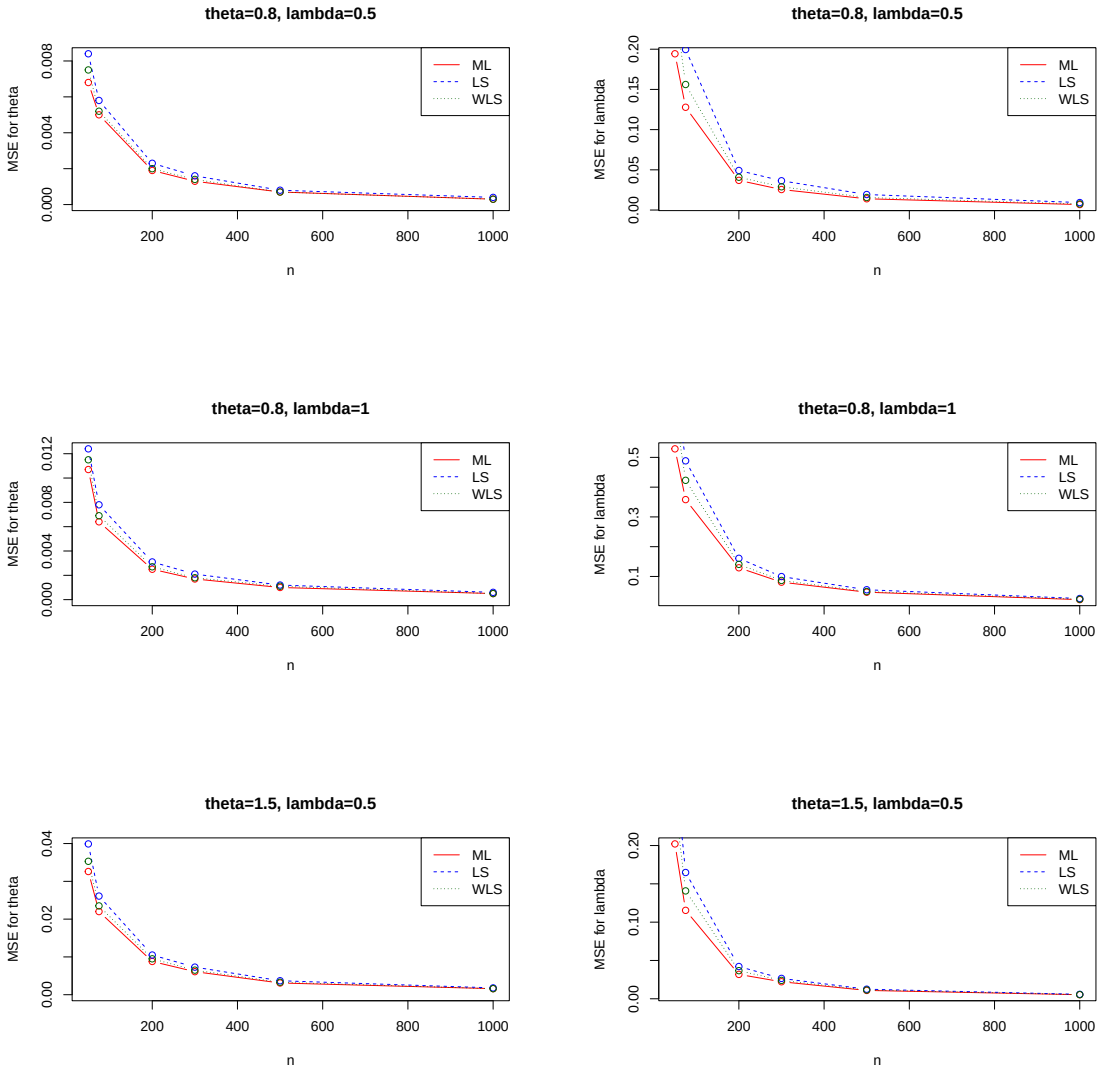
Table 3: Simulation results for WLS estimates, Bias, MSE and RMSE.

n	$\hat{\theta}$	$\hat{\lambda}$	Bias(θ)	Bias(λ)	MSE(θ)	MSE(λ)	RMSE(θ)	RMSE(λ)
			$\theta = 0.8,\ \lambda = 0.5$					
50	0.7929	0.6423	-0.0071	0.1423	0.0075	0.2544	0.0864	0.5044
75	0.7982	0.5813	-0.0018	0.0813	0.0052	0.1561	0.0718	0.3952
200	0.8007	0.5215	0.0007	0.0215	0.0020	0.0408	0.0453	0.2019
300	0.7974	0.5284	-0.0026	0.0284	0.0014	0.0289	0.0376	0.1700
500	0.7996	0.5140	-0.0004	0.0140	0.0007	0.0156	0.0274	0.1251
1000	0.7999	0.5022	-0.0001	0.0022	0.0003	0.0076	0.0184	0.0871
			$\theta = 0.8,\ \lambda = 1.0$					
50	0.7954	1.2166	-0.0046	0.2166	0.0115	0.6595	0.1073	0.8121
75	0.7966	1.1380	-0.0034	0.1380	0.0069	0.4229	0.0829	0.6503
200	0.8025	1.0331	0.0025	0.0331	0.0027	0.1406	0.0524	0.3750
300	0.7995	1.0311	-0.0005	0.0311	0.0018	0.0866	0.0425	0.2944
500	0.8006	1.0173	0.0006	0.0173	0.0011	0.0494	0.0324	0.2223
1000	0.8004	1.0077	0.0004	0.0077	0.0005	0.0234	0.0231	0.1528
			$\theta = 1.5,\ \lambda = 0.5$					
50	1.4797	0.6435	-0.0203	0.1435	0.0353	0.2572	0.1878	0.5072
75	1.4987	0.5778	-0.0013	0.0778	0.0235	0.1408	0.1533	0.3752
200	1.4957	0.5316	-0.0043	0.0316	0.0095	0.0367	0.0973	0.1916
300	1.4995	0.5203	-0.0005	0.0203	0.0065	0.0240	0.0807	0.1548
500	1.5024	0.5097	0.0024	0.0097	0.0033	0.0115	0.0576	0.1074
1000	1.4997	0.5063	-0.0003	0.0063	0.0016	0.0054	0.0404	0.0735
			$\theta = 1.5,\ \lambda = 1.0$					
50	1.4826	1.3142	-0.0174	0.3142	0.0547	0.8339	0.2340	0.9132
75	1.4943	1.2029	-0.0057	0.2029	0.0383	0.5811	0.1957	0.7623
200	1.5015	1.0667	0.0015	0.0667	0.0143	0.1809	0.1104	0.4254
300	1.4980	1.0544	-0.0020	0.0544	0.0095	0.1077	0.0976	0.3282
500	1.4971	1.0417	-0.0029	0.0417	0.0060	0.0674	0.0773	0.2597
1000	1.5018	1.0084	0.0018	0.0084	0.0027	0.0263	0.0520	0.1622

The simulation results indicate that the estimators $\hat{\theta}$ and $\hat{\lambda}$ perform well across different sample sizes. As the sample size n increases, the estimated values $\hat{\theta}$ and $\hat{\lambda}$ tend to approach their respective true parameter values θ and λ, indicating that the estimators exhibit desirable finite-sample properties.

Moreover, the biases associated with both parameter estimators decrease and approach zero as n increases. Similarly, the MSE and RMSE of both $\hat{\theta}$ and $\hat{\lambda}$ exhibit a decreasing trend with increasing sample size. These results indicate improved estimation accuracy and precision as the sample size increases.

Overall, the simulation results suggest that the estimators exhibit desirable finite-sample behavior, with bias, MSE, and RMSE generally decreasing as the sample size increases.



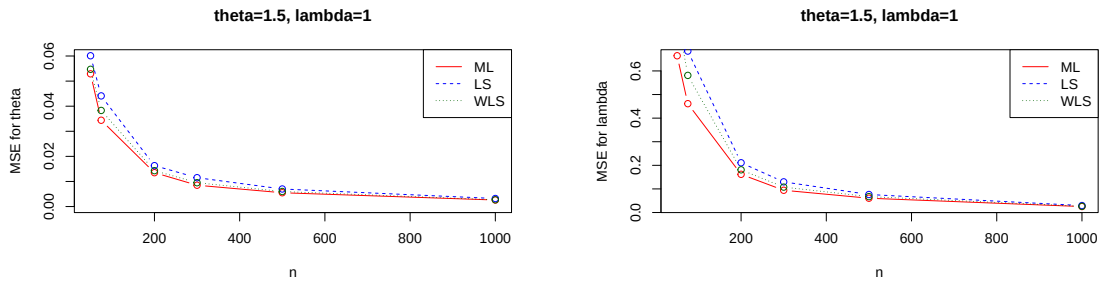


Figure 6: Graphical comparison of the MSEs obtained from ML, OLS, and WLS estimation methods for different parameter combinations.

6 Application

6.1 Methodology

In this section, two real-life datasets are used to demonstrate the advantages of the UTPCJD. After the data were fitted with the UTPCJD, the results were compared with those obtained from other probability distributions specified in the unit interval based on the Akaike information criterion (AIC), corrected Akaike information criterion (AICc), consistent Akaike information criterion (CAIC), and Bayesian information criterion (BIC). In addition, the Kolmogorov–Smirnov (KS) test and the corresponding p-value were used to assess the models' goodness-of-fit.

- $\text{AIC} = 2k - 2\log l.$
- $\text{AICc} = \text{AIC} + \frac{2k(k+1)}{n-k-1}.$
- $\text{CAIC} = -2\log l + k(\log n + 1).$
- $\text{BIC} = k\log n - 2\log l.$

Here, $\log l$ denotes the estimated value of the maximum log-likelihood, k denotes the number of parameters, and n denotes the number of observations. For comparison with the UTPCJD, the following probability distributions defined on the unit interval were considered.

- Beta distribution (BD):

$$f(y:\alpha,\beta) = \frac{y^{\alpha-1}(1-y)^{\beta-1}}{B(\alpha,\beta)}, \quad y \in (0,1),\ \alpha,\beta > 0.$$

- Kumaraswamy distribution (KD) [23]:

$$f(y;\alpha,\beta) = \alpha\beta\, y^{\alpha-1}(1-y^{\alpha})^{\beta-1}, \quad y \in (0,1),\ \alpha,\beta > 0.$$

- Unit Weibull distribution (UWD) [24]:

$$f(y;\alpha,\beta) = \frac{\alpha\beta}{y}(-\ln y)^{\beta-1}\exp\left[-\alpha(-\ln y)^{\beta}\right], \quad y \in (0,1),\ \alpha,\beta > 0.$$

- Log-Lindley distribution (LLD) [25]:

$$f(y;\sigma,\lambda) = \frac{\sigma^2}{1+\lambda\sigma}(\lambda - \ln y)\, y^{\sigma-1}, \quad y \in (0,1),\ \sigma,\lambda > 0.$$

- Exponentiated Topp–Leone distribution (ETLD) [26]:

$$f(y;\alpha,\beta) = 2\beta\alpha(1-y)\, y^{\alpha-1}(2-y)^{\alpha-1}\left[1 - y^{\alpha}(2-y)^{\alpha}\right]^{\beta-1}, \quad y \in (0,1),\ \alpha,\beta > 0.$$

- Unit Burr III distribution (UBD) [27]:

$$f(y;\alpha,\beta) = \frac{\alpha\beta}{y^2}\left(\frac{1-y}{y}\right)^{-\alpha-1}\left[1+\left(\frac{1-y}{y}\right)^{-\alpha}\right]^{-\beta-1}, \quad y \in (0,1),\ \alpha,\beta > 0.$$

6.2 Data Description and Inference

The first dataset [28, 29] relates to a comparison of the SC 16 and P3 unit capacity factor estimation techniques. The data is displayed in Table 4.

Table 4: Observations of Dataset 1

0.853	0.759	0.866	0.809	0.717	0.544	0.492	0.403
0.344	0.213	0.116	0.116	0.092	0.070	0.059	0.048
0.036	0.029	0.021	0.014	0.011	0.008	0.006	

The second dataset [30] comprises the initial 59 observations documenting the time of failure for Kevlar 49/epoxy strands tested at a stress level of 90%. The data is presented in Table 5.

Table 5: Observations of Dataset 2

0.01	0.01	0.02	0.02	0.02	0.03	0.03	0.04	0.05
0.06	0.07	0.07	0.08	0.09	0.09	0.1	0.1	0.11
0.11	0.12	0.13	0.18	0.19	0.2	0.23	0.24	0.24
0.29	0.34	0.35	0.36	0.38	0.4	0.42	0.43	0.52
0.54	0.56	0.6	0.6	0.63	0.65	0.67	0.68	0.72
0.72	0.72	0.73	0.79	0.79	0.8	0.8	0.83	0.85
0.9	0.92	0.95	0.99	0.01				

The results for dataset 1 and dataset 2 are summarized in Tables 6 - 9. These tables specifically provide the log-likelihood (LogL) value, ML estimates, AIC, AICc, CAIC,

BIC, and the value of the KS statistic together with the corresponding p-value for each fitted model. The UTPCJD provides a better fit, as indicated by its smallest values of AIC, AICc, CAIC, and BIC, along with the smallest KS statistic and the largest p-value.

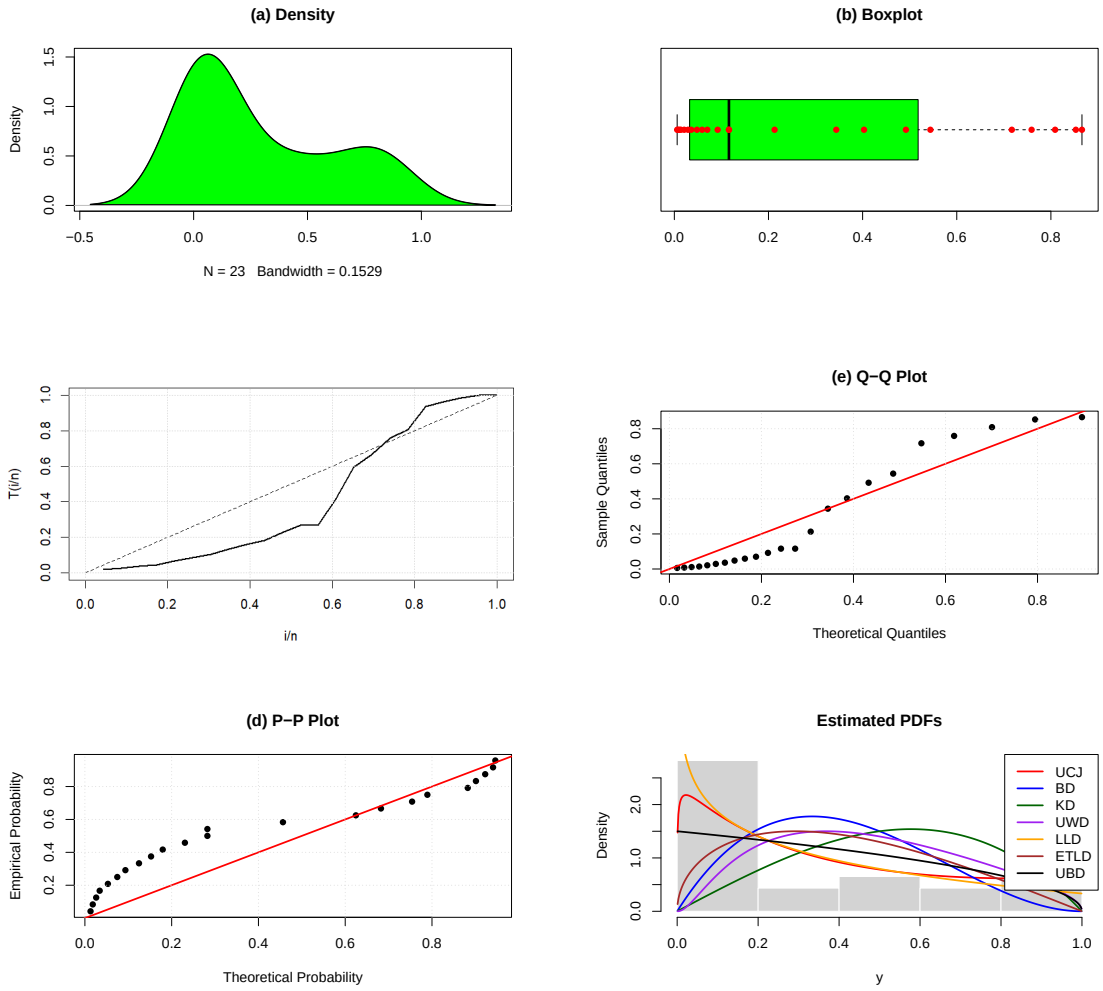


Figure 7: The density, boxplot, TTT, P-P, estimated pdf, and Q-Q plots based on the first dataset.

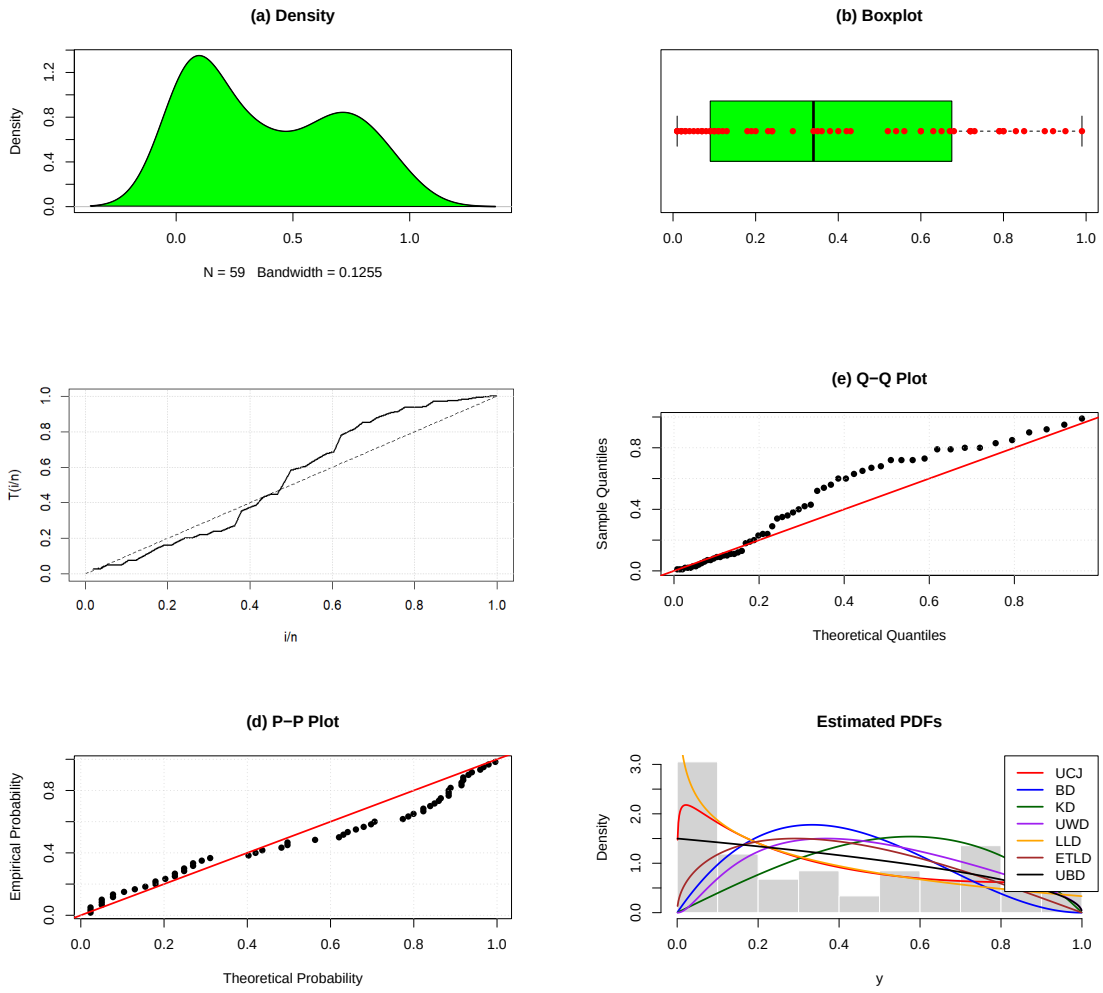


Figure 8: The density, boxplot, TTT, P-P, estimated pdf, and Q-Q plots based on the second dataset.

Table 6: MLE, standard errors, KS and p-values

Distribution	ML Estimates	S.E	KS	p-value
UTPCJD	$\hat{\theta} = 0.9722, \hat{\lambda} = 1.5511$	0.1831, 1.2356	0.1410	0.7503
BD	$\hat{\alpha} = 0.486, \hat{\beta} = 1.167$	0.1208, 0.3578	0.1836	0.4203
KD	$\hat{\alpha} = 0.5044, \hat{\beta} = 1.186$	0.1288, 0.3265	0.1790	0.4529
UBD	$\hat{\alpha} = 0.4536, \hat{\beta} = 1.0015$	0.1348, 0.2515	0.1893	0.3819
UWD	$\hat{\alpha} = 0.3645, \hat{\beta} = 1.1951$	0.1169, 0.2106	0.1635	0.5696
LLD	$\hat{\sigma} = 0.6904, \hat{\lambda} = 1.3380$	0.1742, 1.8762	0.1644	0.5624
ETLD	$\hat{\alpha} = 0.4623, \hat{\beta} = 0.6805$	0.1389, 0.1717	0.1933	0.3562

Table 7: Information criteria

Distribution	LogL	AIC	AICc	CAIC	BIC
UTPCJD	10.8464	-17.6929	-17.0928	-13.4219	-15.4219
BD	9.607	-15.214	-14.614	-10.943	-12.94
KD	9.670	-15.341	-14.741	-11.070	-13.070
UBD	9.4845	-14.969	-14.369	-10.698	-12.698
UWD	9.9631	-15.9262	-15.3262	-11.6552	-13.6552
LLD	9.9936	-15.9872	-15.3872	-11.7162	-13.7162
ETLD	9.3913	-14.7826	-14.1826	-10.5116	-12.5116

Table 8: The ML estimates of the parameters with their standard errors, KS value and the associated p-values

Distribution	ML Estimates	S.E	KS	p-value
UTPCJD	$\hat{\theta} = 1.2013, \hat{\lambda} = 2.1398$	0.1822, 1.3558	0.0809	0.8347
BD	$\hat{\alpha} = 0.6505, \hat{\beta} = 1.0292$	0.1048, 0.1842	0.1023	0.5667
KD	$\hat{\alpha} = 0.6553, \hat{\beta} = 1.0364$	0.105, 0.190	0.1021	0.5699
UBD	$\hat{\alpha} = 0.9783, \hat{\beta} = 0.6508$	0.1338, 0.1061	0.1016	0.5761
UWD	$\hat{\alpha} = 0.6107, \hat{\beta} = 1.0576$	0.0982, 0.1121	0.10999	0.5979
LLD	$\hat{\sigma} = 0.8617, \hat{\lambda} = 2.2029$	0.1867, 2.9131	0.0959	0.6491
ETLD	$\hat{\alpha} = 0.6149, \hat{\beta} = 0.5618$	0.1235, 0.0868	0.1098	0.4743

Table 9: LogL, AIC, AICc, CAIC, BIC for dataset 2

Distribution	LogL	AIC	AICc	CAIC	BIC
UTPCJD	8.1326	-12.2653	-12.0510	-6.1102	-8.1102
BD	6.8353	-9.6707	-9.4564	-3.5156	-5.5156
KD	6.8446	-9.6893	-9.4750	-3.5342	-5.5342
UBD	6.8353	-9.6707	-9.4565	-3.5157	-5.5157
UWD	6.9591	-9.9182	-9.7039	-3.7632	-5.7632
LLD	7.1403	-10.2806	-10.0663	-4.1255	-6.1255
ETLD	6.5722	-9.1445	-8.9302	-2.9894	-4.9894

From the above tables, it is observed that the performance of the considered distributions varies across the datasets. Based on the KS statistic and the corresponding p-values, the UTPCJD provides a good fit to the data, as it has relatively smaller KS values and higher p-values compared to the other models. In contrast, some of the other models show small p-values, indicating a poor fit to the data. This result is further supported by the information criteria values (AIC, AICc, CAIC, and BIC), where the UTPCJD generally attains lower values, suggesting a better model fit. For the second dataset as well, the UTPCJD model continues to show competitive performance. Overall, the results indicate that the UTPCJD provides the best fit among the considered models, while the other distributions show moderate to relatively poorer performance depending on the dataset.

7 Conclusion

In this study, a bounded version of the TPCJD was developed using an exponential transformation, referred to as the UTPCJD. Various statistical properties, including shape behavior, moments, incomplete moments, mgf, HRF and identifiability were derived. Additionally, measures such as Shannon entropy, extropy, and inequality measures were obtained. Parameter estimation was carried out using ML, OLS, and WLS, and their performance was evaluated through simulation studies. The effectiveness of the proposed model was further validated using real datasets. Based on these findings, the UTPCJD proves to be a suitable and flexible model for data defined on the unit interval.

References

[1] Gupta, A. K., Nadarajah, S.: Handbook of Beta Distribution and Its Applications. CRC Press (2004).

[2] Kumaraswamy, P.: A generalized probability density function for double-bounded random processes. *Journal of Hydrology* 46(1–2), 79–88 (1980).

[3] Jones, M. C.: Kumaraswamy's distribution: A beta-type distribution with some tractability advantages. *Statistical Methodology* 6(1), 70–81 (2009).

[4] Bonferroni, Carlo E: Elementi di statistica generale. *Universitacommerciale Bocconi* (1941).

[5] Zenga, Michele and others.: Inequality curve and inequality index based on the ratios between lower and upper arithmetic means. *Vita e pensiero* (2007).

[6] Van der Vaart, Aad W: Asymptotic statistics *Cambridge university press* 3, 70–81 (2000).

[7] Ghitany, M. E., Mazucheli, J., Menezes, A. F. B., Alqallaf, F.: The unit-inverse Gaussian distribution: A new alternative to two-parameter distributions on the unit interval. *Communications in Statistics – Theory and Methods* 48(14), 3423–3438 (2019).

[8] Maya, R., Jodrá, P., Irshad, M. R., Krishna, A.: The unit Muth distribution: Statistical properties and applications. *Ricerche di Matematica* 73(4), 1843–1866 (2024).

[9] Krishna, A., Maya, R., Chesneau, C., Irshad, M. R.: The unit Teissier distribution and its applications. *Mathematics and Computational Applications* 27(1), 12 (2022).

[10] Al-Moisheer, A. S., Sultan, K. S., Mansour, M. M. M., Nagaty, H.: Unit linear failure rate distribution with applications in socioeconomic and reliability data. *Symmetry* 18(4), 554 (2026).

[11] Sarhan, A. M., Manshi, T. S., Sobh, M. E.: The unit-modified Weibull distribution: Theory, estimation, and real-world applications. *Stats* 8(3), 81 (2025).

[12] Sarhan, A. M.: Unit-Chen distribution and its quantile regression model with applications. *Scientific African* 27, e02555 (2025).

[13] Chinedu, E. Q., Chukwudum, Q. C., Alsadat, N., Obulezi, O. J., Almetwally, E. M., Tolba, A. H.: New lifetime distribution with applications to single acceptance sampling plan and scenarios of increasing hazard rates. *Symmetry* 15(10), 1881 (2023).

[14] Onyekwere, C. K., Obulezi, O. J.: Chris-Jerry distribution and its applications. *Asian Journal of Probability and Statistics* 20(1), 16–30 (2022).

[15] Irshad, M. R., Aswathy, S., Chesneau, C., Maya, R.: CUSUM control chart for monitoring mean of the INAR (1) PCJ process. *Model Assisted Statistics and Applications* 20(1), 20–37 (2025).

[16] Ibeakuzie, P. O., Anabike, I. C., Nwankwo, P. M., Chinedu, E. Q., Ekemezie, D. F. N., Igbokwe, C. P.: Generalized weighted Chris-Jerry distribution: Properties and applications. *Complexity Analysis and Applications* 1(1), 30–44 (2024).

[17] Korkmaz, M. C.: The unit generalized half normal distribution: A new bounded distribution with inference and application. (2020).

[18] Herzallah, A. M., Al-Moisheer, A. S., Sultan, K. S.: A novel unit exponential delay time distribution: Theory, inference and applications. *Mathematics* 14(6), 1029 (2026).

[19] Al-Moisheer, A. S., Sultan, K. S., Mansour, M. M. M.: On unit J-shaped distributions: Properties and estimation with applications. *Mathematics* 14(6), 1021 (2026).

[20] Zhang, T., Xie, M., Tang, L. C., Ng, S. H.: Reliability and modeling of systems integrated with firmware and hardware. *International Journal of Reliability, Quality and Safety Engineering* 12(3), 227–239 (2005).

[21] Shannon, C. E.: A mathematical theory of communication. *Bell System Technical Journal* 27(3), 379–423 (1948).

[22] Lad, F., Sanfilippo, G., Agro, G.: Extropy: Complementary dual of entropy. *Statistical Science* 30(1), 40–58 (2015).

[23] Badr, D. H., Mohammed, M. A. H.: The Kumaraswamy distribution: Statistical properties and application. *International Journal of Advanced Science, Engineering and Information Technology* 12, 1–7 (2022).

[24] Mazucheli, J., Menezes, A. F. B., Ghitany, M. E.: The unit-Weibull distribution and associated inference. *Journal of Applied Probability and Statistics* 13(3), 1–18 (2018).

[25] Gómez-Déniz, E., Sordo, M. A., Calderín-Ojeda, E.: The Log–Lindley distribution as an alternative to the beta regression model with applications in insurance. *Insurance: Mathematics and Economics* 54, 49–57 (2014).

[26] Pourdarvish, A., MirMostafaee, S. M. T., Naderi, K.: The exponentiated Topp–Leone distribution: Properties and application. *Journal of Applied Environmental and Biological Sciences* 5(7), 251–256 (2015).

[27] Modi, K., Gill, V.: Unit Burr-III distribution with application. *Journal of Statistics and Management Systems* 23(3), 579–592 (2020).

[28] Caramanis, M., Stremel, J., Fleck, W., Daniel, S.: Probabilistic production costing: An investigation of alternative algorithms. *International Journal of Electrical Power & Energy Systems* 5(2), 75–86 (1983).

[29] Mazumdar, M., Gaver, D. P.: On the computation of power-generating system reliability indexes. *Technometrics* 26(2), 173–185 (1984).

[30] Sudsila, P., Thongteeraparp, A., Aryuyuen, S., Bodhisuwan, W.: The generalized distributions on the unit interval based on the T-Topp-Leone family of distributions. *Trends Sci* 19(19), 6186 (2022).